Optics and Photonics Journal, 2016, 6, 136-144
Published Online August 2016 in SciRes. http://www.scirp.org/journal/opj
http://dx.doi.org/10.4236/opj.2016.68B023

Analysis of Optical Properties of Off-Axis Reflective Volume Holographic Grating

Zhenmin Shen*, Weidong Shang, Yuzhao Wang, Long Gao, Yuliang Tao, Jukui Yang

Laboratory of Laser Engineering and Technology, Beijing Institute of Space Mechanics & Electricity, Beijing, China
Email: *szm@bit.edu.cn

Received 8 July 2016; accepted 18 August 2016; published 25 August 2016

Abstract

The coupled wave theory for volume holographic grating with curved interference fringes has been proposed based on the Kogelnik's coupled wave theory with the plane interference fringes. The formula about the magnitude and directional angle of grating vector in arbitrary position of volume holographic grating with curved grating has been deduced. We found that the wavelength selectivity and angular selectivity may be different in different position of volume holographic curved stripe grating which depend on the angle between the propagation vector of reference beam and signal beam. The larger the angle, the greater the angle and wavelength selectivity, whereas the weaker.

Keywords

Volume Holographic Grating, Couple Wave Theory, Interference Fringe

1. Introduction

In 1948, Dennis Gabor proposed the holographic wavefront reconstruction technique to reduce the aberration of electron microscopy and improve the image resolution, namely, the short wavelength electromagnetic spectrum line was used to store the measured object image, while the long wavelength electromagnetic spectrum was used to reproduce. In the field of holographic optical, holographic wavefront reconstruction is to use two beams of coherent light exposure holographic material, and the interference fringes of two beams of coherent light will be recorded in holographic material, and any beam at the original records is used to irradiate the recorded holographic material, which can reproduce another beam at the original records [1]-[6].

If the object and reference beams are both point light source and recorded in the holographic medium, the holographic medium consisting of point source hologram can be as the basic holographic optical element, which can be realized the function of the basic lens, a reflecting mirror. A point source of holographic optical elements can be a bunch of diverging or converging spherical wave and a bunch of planar light wave mutual interference, and can also two beams of spherical waves interfere with each other, or two beams of plane waves interfere with each other. The interference fringes can be a group of paraboloid, ellipsoid, hyperboloid or plane, depending on two point light source with respect to the position of the plane of the recording medium position [7]-[12].

*Corresponding author.

How to cite this paper: Shen, Z.M., Shang, W.D., Wang, Y.Z., Gao, L., Tao, Y.L. and Yang, J.K. (2016) Analysis of Optical Properties of Off-Axis Reflective Volume Holographic Grating. *Optics and Photonics Journal*, **6**, 136-144.
http://dx.doi.org/10.4236/opj.2016.68B023

2. Interference Field of Plane Wave and Converging Spherical Wave

According to the theory of holographic wavefront reconstruction, when object beam with the convergent spherical wave and reference beam with the parallel light is used to exposure to holographic media at different side, the converging spherical wave can be reconstruction by irradiating the reference beam on the redording holographic media, which achieves the function of focusing mirror.

The expression of complex amplitude E_1 and E_2 of two coherent light waves are respectively [13]:

$$E_1 = A_1 \exp(\mathrm{j}\, k_0 L_1) \tag{1}$$

$$E_2 = A_2 \exp(\mathrm{j}\, k_0 L_2) \tag{2}$$

where A_1 and A_2 are respectively the amplitude of light wave of E_1 and E_2; k_0 is the wave vector in the vacuum, and $k_0 = 2\pi / \lambda_0$, λ_0 is the wavelength of light in the vacuum; L_1 and L_2 are respectively the light path of two beams.

According to the interference principle, the two light waves meet with the same frequency, same vibration direction, which would produce interference phenomenon The distribution of the interference intensity is:

$$I = A_1^2 + A_2^2 + 2A_1A_2 \cos k_0(L_1 - L_2) \tag{3}$$

When the optical path difference is equal to the wavelength of integer times, that is $L_1 - L_2 = m\lambda_0$, the position would have the constructive inference.

Assuming that a converging spherical wave E_1 gathers the origin of coordinates, and the propagation direction of another plane wave E_2 parallels to the YZ plane with the angle θ_1 for the z axis. Thus, $L_1 = -n\sqrt{x^2 + y^2 + z^2}$ and $L_2 = n(z\cos\theta_1 + y\sin\theta_1)$. The the location generating an constructive interference is:

$$n\left(-\sqrt{x^2 + y^2 + z^2} - z\cos\theta_1 - y\sin\theta_1\right) = m\lambda_0 \qquad (m \le 0) \tag{4}$$

From the Formula (4), we can see that the position of constructive interference is a group of paraboloid of revolution, which is symmetry with the beeline of $y = z\tan\theta_1$, but the opening towards the propagation of plane waves in the opposite direction. When the angle θ_1 between the parallel optical wave and the Z axis is zero, the pattern generating the constructive interference in the YZ plane is a parabolic, as shown in **Figure 1**. The parabola opening is in the negative direction of the Z axis. With the increase of the absolute value of the interference level *m*, the parabola opening is gradually increased. The maximum interference level is the zero, and the position of constructive interference is non positive part of the Z axis, and the minimum interference level is negative infinity. For a certain level *m* of interference, the parabolic peak is located at the Z axis of the $-m\lambda_0 / 2n$, and the distance of the parabolic peak between the adjacent interference level is $\lambda_0 / 2n$.

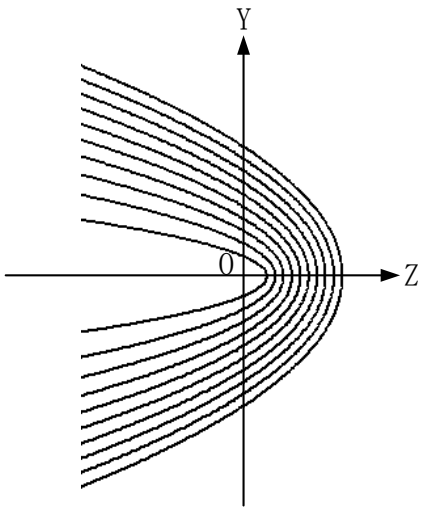

Figure 1. Interference field of plane wave and converging spherical wave.

3. The "Curved" Coupled Wave Theory Based on "Plane" Coupled Wave Theory

In the last section, the interference fringes are formed by the signal beam and the reference beam in the holographic material, which is the basic holographic optical element, and can be called as the holographic grating [14]. According to the comparison of the thickness of the holographic recording medium and the fringe spacing of the recording, the holographic grating can be divided into volume holographic grating (thick holographic grating) or plane holographic grating (thin holographic grating). If the thickness of the holographic recording medium is equal to or greater than the recorded interference fringe interval, the interference fringe formed in the recording medium is three-dimensional distribution, namely the volume holographic grating. Due to high diffraction efficiency of volume holographic grating, so that the volume holographic optical elements are widely used in many optical system. The volume holographic optical elements at the incidence of the Bragg angle or close to the Bragg angle can obtain effective wavefront reconstruction [15]-[18].

The interference fringes formed by point source hologram in holographic medium can be divided into two kinds: the plane interference fringe and the curved interference fringe. In holographic interferogram for point source field, the only the interference fringes of one plane wave and another plane wave are planar shape. When a convergent spherical wave or divergent spherical wave is the reference beam or the signal beam, the interference fringes formed by the interference field are curved shape (paraboloid, hyperboloid, ellipsoid). The coupled wave theory proposed by Kogelnik in 1969 mainly analyzed the characteristic of the holographic grating with plane interference fringes, not analyzed the holographic grating with curved interference fringes.

Therefore, the "curved" coupled wave theory is derived in this paper, based on the "plane" coupled wave theory. The geometric structures of the base element hologram are respectively recorded by the two plane waves and the converging spherical wave and plane wave as shown in **Figure 2** and **Figure 3**. By comparison, the direction and magnitude of grating vector $\boldsymbol{k}_{\mathbf{F}}$ of volume hologram recorded by two plane waves are both the same in the whole position in **Figure 2**, in other words, the direction and magnitude of grating vector is a constant ϕ. But the grating vector $\boldsymbol{k}_{\mathbf{F}}$ recorded by converging spherical wave and plane wave may be different in different position, that is, ϕ is variable.

According to the wave differential equation, after a series of deduction, the diffraction efficiency of the holographic grating is described as [15]

$$\eta = 1 \Big/ \left\{ 1 + \left(1 - \xi^2 / \nu^2\right) \Big/ \mathrm{sh}^2\left(\nu^2 - \xi^2\right)^{\frac{1}{2}} \right\} \tag{5}$$

Here,

$$\nu = j\pi n_1 d \Big/ \lambda \left(c_R c_S\right)^{\frac{1}{2}} \tag{6}$$

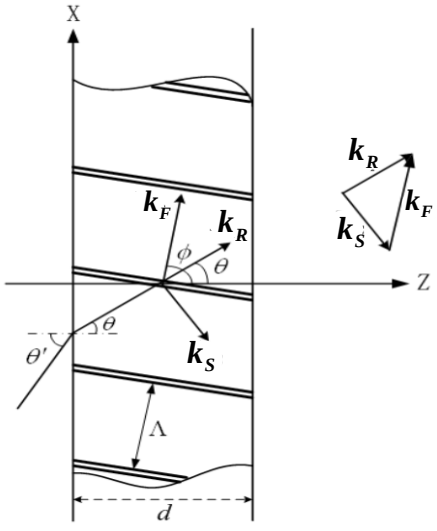

Figure 2. The volume holographic grating recorded by two plane waves.

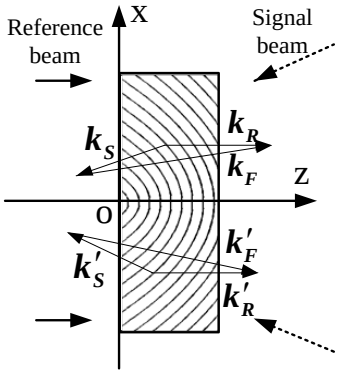

Figure 3. The volume holographic grating recorded by converging spherical wave and plane wave.

$$\xi = -\vartheta d / 2c_S \tag{7}$$

where, n_1 is the refractive index of volume holographic grating, d is the thickness of volume holographic grating, is the incident light wavelength for reconstruction, c_R and c_S are the inclination factor of volume holographic grating, and can be described as:

$$c_R = k_{Rz} / k_R = \cos\theta \tag{8}$$

$$c_S = k_{Sz} / k_S = \cos\theta - \frac{k_F}{k_R}\cos\phi \tag{9}$$

where $\boldsymbol{k_F}$ is the grating vector of volume hologram, $\boldsymbol{k_R}$ is wave vector of reference beam, θ is the angle between the reference beam and the z aixs, and ϕ is the angle between the grating vector and the z axis.

In the Formula (7), ϑ is described as:

$$\vartheta = k_F \cos(\phi - \theta) - \frac{k_F^2}{4\pi n}\lambda \tag{10}$$

where n is the average refractive index of volume holographic grating.

If the incident angle θ of reference wave deviates from the Bragg angle of $\Delta\theta$, the incident angle can be described as $\theta = \theta_0 + \Delta\theta$. If the wavelength of reference wave deviates from the recording wavelength, the wavelength can be described as $\lambda = \lambda_0 + \Delta\lambda$. Thus, the Formula (10) can be described as

$$\vartheta = k_F \sin(\phi - \theta_0)\sin(\Delta\theta) - \frac{k_F^2}{4\pi n}\Delta\lambda + \frac{k_F^2\lambda_0}{4\pi n}\left[\cos(\Delta\theta) - 1\right] \tag{11}$$

When $\Delta\theta$ is little, the Formula (11) can be described as:

$$\vartheta = \Delta\theta k_F \sin(\phi - \theta_0) - \Delta\lambda\frac{k_F^2}{4\pi n} \tag{12}$$

Kogelnik only analyzed the diffraction efficiency of volume holographic grating under the condition of the interference fringes are the plane by the interference of two plan waves, that is, the size k_F and angle ϕ of grating vector are the same in the whole position of grating. But the k_F and ϕ is different in the volume holographic grating with the curved interference fringes, so the wavelength selectivity, the angle selectivity and the diffraction efficiency at arbitrary position of grating may be different. Therefore, the size and direction of the grating vector with curved interference fringes at different locations need to be given.

Assuming that the plane wave (reference beam) is incident to the holographic media from the air with the angle of θ', and the propagation angle in media is θ, and the coordinate of the converging point of spherical wave is (x_S, z_S), and the propagation angle of signal beam in media is φ, and the exit angle from the media into the air is φ', and the coordinate of arbitrary position in media is (x_F, z_F). Therefore, according to the theory of **K** vector closure, it can be deduced that the angle ϕ and size k_F of grating vector at any point in the holographic grating with curved interference fringes.

For the volume holographic grating of the reflection type with the curved interference fringes, the ϕ and k_F are described as:

$$\phi = \frac{1}{2}\left[\theta + \arctan\left(\frac{x_S - x_F}{z_S - z_F}\right)\right] \tag{13}$$

$$k_F = 2\beta\cos\left[\frac{1}{2}\left(\theta - \arctan\left(\frac{x_S - x_F}{z_S - z_F}\right)\right)\right] \tag{14}$$

4. The Optical Properties of the Off-Axis Volume Holographic Grating

The phase volume holographic grating for reflection type and no absorption with the curved interference fringes is divided into the coaxial and off-axis recordings. The reconstruction process is shown in **Figure 4(a)** and **Figure 4(b)**, respectively.

Due to the surface position z_F of the reflection volume holographic grating is zero, only need to analyze the characteristics of the grating when $z_F = 0$ at different locations of x_F.

In **Figure 4(b)**, assuming that the laser wavelength is 532 nm, the coordinate of the converging point of spherical wave is $(x_S, z_S) = (15, -5)$ cm, the incident angle of plane wave is $\theta' = 45^\circ$, the range of coordinate position of holographic media is $x_F = -10 \sim 10$ cm, $z_F = 0 \sim d$ cm.

4.1. Angular Selectivity at Different Locations of the Volume Holographic Grating

The angular selectivity in different locations of x_F for the reflection volume holographic grating with the curved interference fringes is shown in **Figure 5**, when x_F = −10 - 10 cm, z_F = 0 cm, and the thickness of grating is 20 μm, 60 μm, 100 μm, respectively.

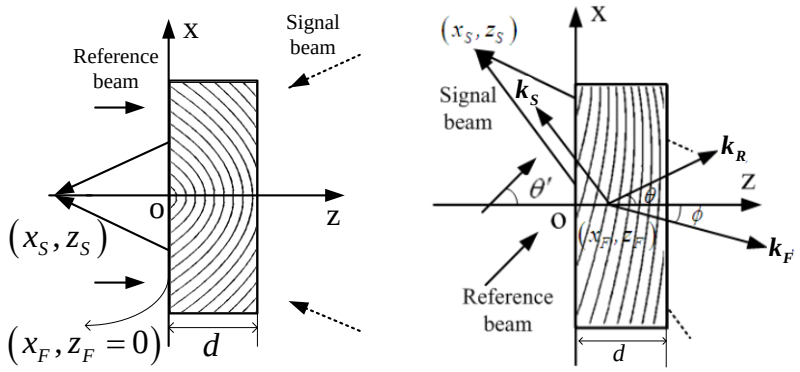

(a) (b)

Figure 4. The sketch of reconstruction process of reflection volume holographic grating with the curved interference fringes recorded by the plane wave and the converging spherical wave. (a) the coaxial recording; (b) the off-axis recording.

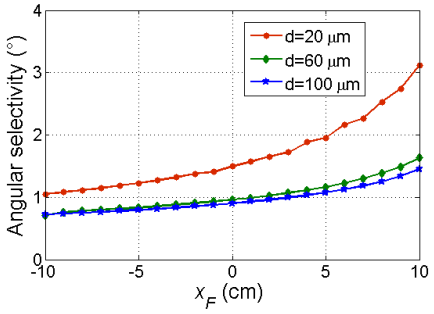

Figure 5. The angular selectivity of reflection volume holographic grating of different thickness at different locations in the off-axis recording($n = 1.5$, $n_1 = 0.01$, $\lambda = 532$nm).

For a certain thickness, the angular selectivity is gradually reduced and the field of view is gradually increased from x_F = −10 - 10 cm. The cause is the increase of the angle between the propagation vector $\boldsymbol{k_R}$ of reference beam and the propagation vector $\boldsymbol{k_S}$ vector of signal beam. The relationship between angular selectivity and diffraction efficiency in the center and two edges of off-axis reflection volume holographic grating with the curved interference fringes is shown in **Figure 6**.

4.2. Wavelength Selectivity at Different Locations of the Volume Holographic Grating

The wavelength selectivity at different locations of off-axis volume holographic grating with the reflection type is shown in **Figure 7**. With the increase of the thickness of grating, the wavelength selectivity will enhance. The relationship between spectral selectivity and diffraction efficiency of in the center and two edges of off-axis reflection volume holographic grating with the curved interference fringes is shown in **Figure 8**.

4.3. Diffraction Efficiency at Different Locations on the Surface of the Grating

In the off-axis records, on the surface of holographic media with x_F = −10 - 10 cm, z_F = 0 cm, and the thickness of holographic media is respectively 20 μm, 60 μm and 100 μm, the diffraction efficiency of the reflection type volume holographic grating with curved interference fringes at different locations of x_F is shown in **Figure 9**, when Bragg angle and recording wavelength is used to reconstruct.

When the thickness of grating is 20 μm, the diffraction efficiency is gradually reduced from x_F = −10 - 10 cm. This is due to the gradual increase of the angle between the propagation vector $\boldsymbol{k_R}$ of the reference beam and the propagation vector $\boldsymbol{k_S}$ of the signal beam in the off-axis recording.

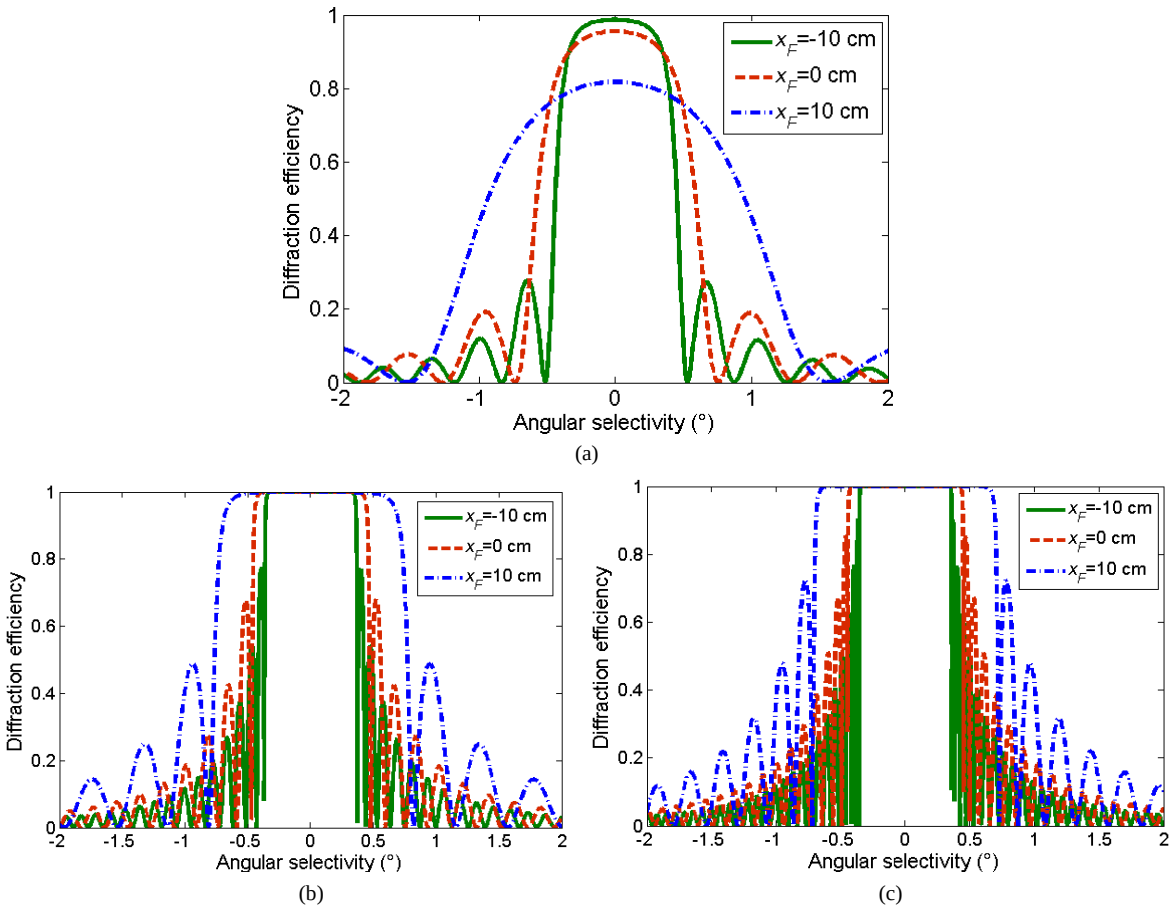

Figure 6. The relationship between angle selectivity and diffraction efficiency of the off-axis recording volume holographic grating with the reflection type. ($n = 1.5$, $n_1 = 0.01$, $\lambda = 532\text{nm}$). (a) d = 20 μm; (b) d = 60 μm; (c) d = 100 μm.

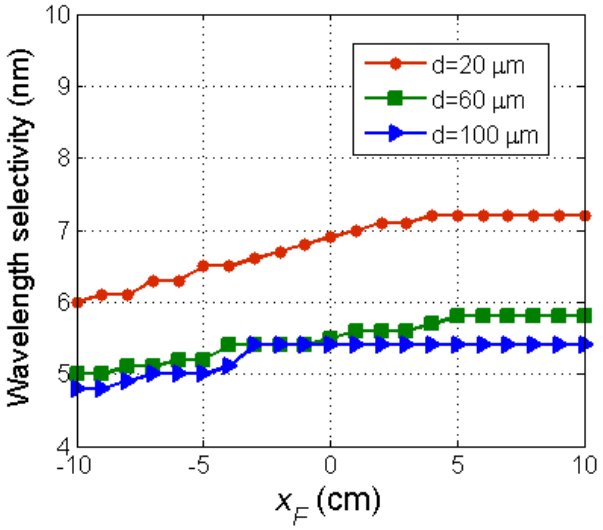

Figure 7. The wavelength selectivity of reflection volume holographic grating of different thickness at different locations in the off-axis recording ($n=1.5$, $n_1=0.01$, $\lambda=532\text{nm}$).

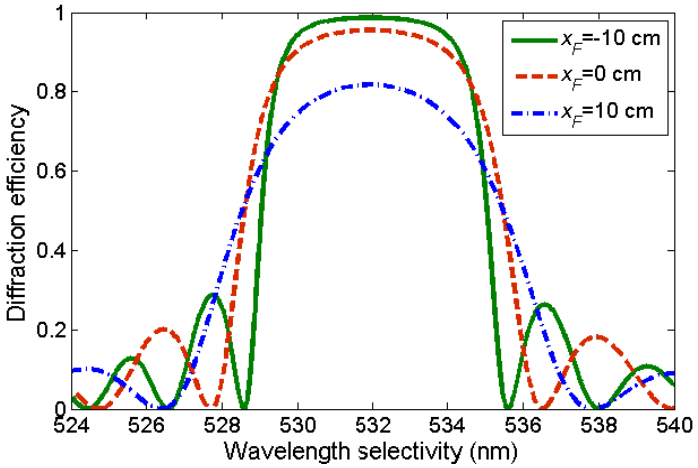

(a)

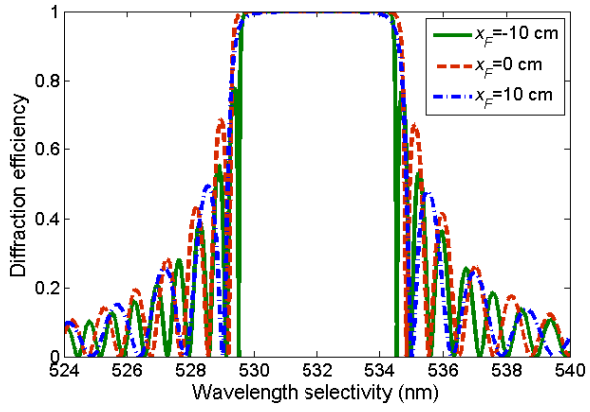

(b)

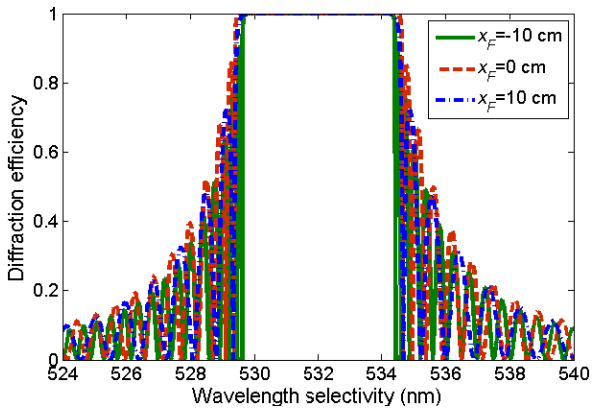

(c)

Figure 8. The relationship between spectral selectivity and diffraction efficiency of the off-axis recording volume holographic grating with the reflection type. ($n=1.5$, $n_1=0.01$, $\lambda=532\text{nm}$).

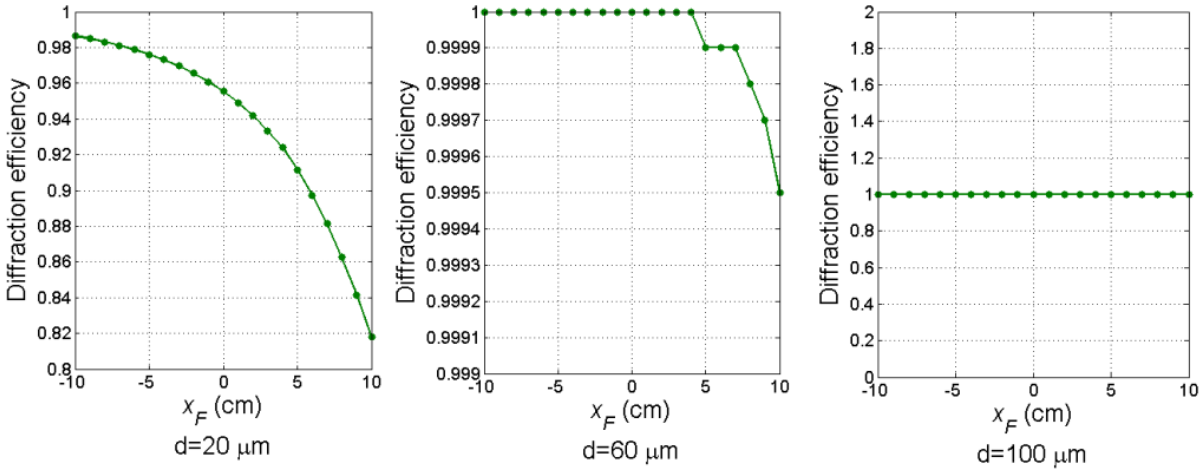

(a) (b) (c)

Figure 9. The diffraction efficiency of reflection volume holographic grating of different thickness at different locations in the off-axis recording ($n=1.5$, $n_1=0.01$, $\lambda=532\text{nm}$).

When the thickness of grating is 60 μm, the diffraction efficiency decreases from 100% to 99.95%.

When the thickness is 100 μm, the diffraction efficiency is 100%, which indicates that the diffraction efficiency is mainly determined by the thickness of the recording medium, and to a certain extent the angle between the propagation vector of light wave affects the diffraction efficiency.

5. Conclusion

Based on the above analysis, the angular and spectral selectivity of reflection type volume holographic grating at different locations is determined by the angle between the propagation vectors of reference beam $\boldsymbol{k_R}$ and signal beam $\boldsymbol{k_S}$. The smaller the angle, the angular and spectral selection is stronger; the angle becomes larger, the angular and spectral selectivity weaker. The diffraction efficiency also meet the above conclusions for the relatively thin volume holographic grating, but the diffraction efficiency will be 100% for the relatively thick volume holographic grating.

References

[1] Sweatt, W.C. (1977) Describing Holographic Optical Elements as Lenses. *JOSA*, **67**, 803-808. http://dx.doi.org/10.1364/JOSA.67.000803

[2] Collier, R.J., Burckhardt, C.B. and Lin, L.H. (2006) Optical Holography (Academic, New York, 1971). *Chap*, **9**, 246-250.

[3] Syms, R.R.A., Shamonina, E., Kalinin, V., *et al*. (2005) A Theory of Metamaterials Based on Periodically Loaded Transmission Lines: Interaction between Magnetoinductive and Electromagnetic Waves. *Journal of Applied Physics*, **97**, 064909. http://dx.doi.org/10.1063/1.1850182

[4] Moharam, M.G. and Gaylord, T.K. (1981) Rigorous Coupled-Wave Analysis of Planar-Grating Diffraction. *JOSA*, **71**, 811-818. http://dx.doi.org/10.1364/JOSA.71.000811

[5] Rasanen, J.T., Silvennoinen, R.V.J., Peiponen, K.E., *et al*. (1995) Optical Sensing of Surface Roughness and Waviness by a Computer-Generated Hologram. *Optical Engineering*, **34**, 2574-2580. http://dx.doi.org/10.1117/12.208093

[6] Johnson, K.D. and Dravid, V.P. (1999) Grain Boundary Barrier Breakdown in Niobium Donor Doped Strontium Titanate Using *In Situ* Electron Holography. *Applied Physics Letters*, **74**, 621-623. http://dx.doi.org/10.1063/1.123184

[7] Case, S.K. (1976) Multiple Exposure Holography in Volume Materials.

[8] Mandelkorn, F. (1973) Simple Lens-System Models for Holographic Techniques. *JOSA*, **63**, 1119-1124. http://dx.doi.org/10.1364/JOSA.63.001119

[9] Lukosz, W. (1968) Equivalent-Lens Theory of Holographic Imaging. *JOSA*, **58**, 1084-1091. http://dx.doi.org/10.1364/JOSA.58.001084

[10] Tolstik, E., Winkler, A., Matusevich, V., *et al.* (2009) PMMA-PQ Photopolymers for Head-Up-Displays. *Photonics*

Technology Letters, **21**, 784-786. http://dx.doi.org/10.1109/LPT.2009.2018133

[11] Zhao, H. and Wang, H.J. (2015) Test of Super Larger Optical Remote Sensor by Sub-Aperture Stitching Interferometry. Spacecraft Recovery & Remote Sensing, **36**, 39-45.

[12] Liu, H., Zhou, Y.M. and Jiang, Y.S. (2013) Research and Application of Foreign Space Mirror Materis. *Spacecraft Recovery & Remote Sensing*, **34**, 90-98.

[13] Ohe, Y., Kume, M., Demachi, Y., *et al*. (1999) Application of a Novel Photopolymer to a Holographic Head-Up Display. *Polymers for Advanced Technologies*, **10**, 544-553. http://dx.doi.org/10.1002/(SICI)1099-1581(199909)10:9<544::AID-PAT907>3.0.CO;2-7

[14] Pramitha, V. (2010) A New Metal Ion Doped Panchromatic Photopolymer for Holographic Applications. Cochin University of Science and Technology.

[15] Offner, A. (1966) Ray Tracing through a Holographic System. *JOSA*, **56**, 1509-1512. http://dx.doi.org/10.1364/JOSA.56.001509

[16] Latta, M.R. and Pole, R.V. (1979) Design Techniques for Forming 488-nm Holographic Lenses with Reconstruction at 633 nm. *Applied Optics*, **18**, 2418-2421. http://dx.doi.org/10.1364/AO.18.002418

[17] Latta, J.N. (1971) Computer-Based Analysis of Holography Using Ray Tracing. *Applied Optics*, **10**, 2698-2710. http://dx.doi.org/10.1364/AO.10.002698

[18] Offner, A. (1966) Ray Tracing through a Holographic System. *JOSA*, **56**, 1509-1512.